

## Low-frequency noise in AlTiO/AlGaN/GaN metal-insulator-semiconductor heterojunction field-effect transistors

S. P. Le, T. Ui, T. Q. Nguyen, H.-A. Shih, and T. Suzuki\*

*Center for Nano Materials and Technology, Japan Advanced Institute of Science and Technology (JAIST)  
1-1 Asahidai, Nomi, Ishikawa 923-1292, Japan \*E-mail: tosikazu@jaist.ac.jp, Phone: +81-761-51-1441*

**Abstract** – We investigated low-frequency noise (LFN) in AlTiO/AlGaN/GaN metal-insulator-semiconductor heterojunction field-effect transistors (MIS-HFETs). For gate biases well above the threshold voltage, ordinary  $1/f$  LFN spectra were observed as in the case of Schottky-HFETs. In contrast, near the threshold voltage, we found spectra composed of two Lorentzians with two time constants, which are never observed in Schottky-HFETs. The two time constants are independent of the gate biases and attributed to electron traps in the AlTiO.

### 1 Introduction

GaN-based metal-insulator-semiconductor heterojunction field-effect transistors (MIS-HFETs) have been extensively developed owing to the merits of gate leakage reduction and passivation effects. As a gate insulator, high-dielectric-constant (high- $k$ ) materials, such as  $\text{Al}_2\text{O}_3$  [1],  $\text{HfO}_2$  [2],  $\text{TiO}_2$  [3],  $\text{AlN}$  [4, 5], and  $\text{BN}$  [6], were employed. Furthermore, AlTiO, alloys of  $\text{TiO}_2$  and  $\text{Al}_2\text{O}_3$ , is one of promising insulators [7], because we can balance the dielectric constant  $k$  and the bandgap  $E_g$  by choosing intermediate properties between  $\text{TiO}_2$  ( $k \sim 60$ ,  $E_g \sim 3$  eV) and  $\text{Al}_2\text{O}_3$  ( $k \sim 9$ ,  $E_g \sim 7$  eV) [8]. In this work, we fabricated AlTiO/AlGaN/GaN MIS-HFETs with an  $\text{Al}_x\text{Ti}_y\text{O}$  ( $x : y = 0.73 : 0.27$ ) gate insulator deposited by atomic layer deposition (ALD), and systematically characterized LFN in the MIS-HFETs. As a result, we found a specific LFN behavior due to the AlTiO gate insulator.

### 2 Device fabrication and DC characterization

On  $\text{Al}_{0.27}\text{Ga}_{0.73}\text{N}(30 \text{ nm})/\text{GaN}(3000 \text{ nm})$  heterostructure obtained by metal-organic vapor phase epitaxy on sapphire(0001), Ti/Al/Ti/Au Ohmic electrodes were formed and device isolation was achieved by  $\text{B}^+$  implantation. A 29-nm-thick  $\text{Al}_x\text{Ti}_y\text{O}$  ( $x : y = 0.73 : 0.27$ ) film as the gate insulator was deposited on the AlGaN surface by ALD using trimethylaluminum (TMA), tetrakisdimethylamino titanium (TDMAT), and  $\text{H}_2\text{O}$  as precursors, where we obtain  $k \sim 13$ ,  $E_g \sim 6$  eV, and the breakdown field  $\sim 6.5$  MV/cm of the AlTiO layer. After formation of Ni/Au gate electrodes on the AlTiO layer, a post-gate-deposition annealing completed the device fabrication. The MIS-HFETs have gate length  $L_G = 0.26, 0.56$ , and  $1.1 \mu\text{m}$ , gate width  $W = 50 \mu\text{m}$ , source-gate spacing  $2 \mu\text{m}$ , and gate-drain spacing  $3 \mu\text{m}$ . We obtained simultaneously two-terminal (2T) ungated devices with electrode spacing  $L = 2\text{-}16 \mu\text{m}$  and width  $W = 100 \mu\text{m}$ . Output and transfer characteristics of the MIS-HFET with the gate length  $L_G = 0.26 \mu\text{m}$  are shown in Fig. 1. High drain currents and transconductances are obtained. In addition, we obtain low gate currents indicating good insulating properties of the AlTiO gate insulator.

### 3 LFN characterization

LFN in the 2T ungated devices is shown in Fig. 2, exhibiting the current noise power spectrum density (PSD)  $S_I \simeq KI^2/f$  with the current  $I$ , the frequency  $f$ , and a constant factor  $K$ , where  $I$  is varied by changing the voltage  $V$ . The Hooge parameter  $\alpha \sim 4 \times 10^{-4}$  of the ungated part with AlTiO is extracted, while the ungated part without AlTiO gives  $\alpha \sim 5 \times 10^{-4}$ . The Hooge parameter  $\alpha$ , the mobility  $\mu$ , and the sheet electron concentration  $n_s$  for the ungated region with and without AlTiO are summarized in Table 1, showing similar results for both cases.

Figure 3 shows the drain current noise PSD  $S_{I_D}$  for the linear regime of the MIS-HFETs with the gate length  $L_G = 0.26 \mu\text{m}$  under the fixed gate voltages  $V_G$ . We confirm the relation  $S_{I_D} \propto I_D^2$ , where the drain current  $I_D$  is varied by changing the drain voltage  $V_D$ . For gate biases well above the threshold voltage,  $V_G \gtrsim -4$  V, ordinary  $1/f$  LFN spectra satisfying  $S_{I_D} \simeq K_{\text{HFET}}I_D^2/f$  with a constant factor  $K_{\text{HFET}}$ , were obtained as shown in Fig. 3 (a). In contrast, near the threshold voltage,  $-7 \text{ V} \lesssim V_G \lesssim -5 \text{ V}$ , we found non- $1/f$  LFN spectra as shown in Fig. 3 (b), where the contribution from the extrinsic ungated part is negligible as confirmed by an analysis of the ungated devices [9]. As shown by the curves in Fig. 3 (b), the non- $1/f$  spectra can be well-fitted by two Lorentzians

$$\frac{S_{I_D}(f)}{I_D^2} = \frac{A_1}{1 + (2\pi f\tau_1)^2} + \frac{A_2}{1 + (2\pi f\tau_2)^2} \quad (1)$$

with prefactors  $A_1$  and  $A_2$ , and time constants  $\tau_1$  and  $\tau_2$ . Since such Lorentzian spectra are not observed in the AlN/AlGaN/GaN MIS-HFETs as well as AlGaN/GaN Schottky-HFETs [9, 10], they are attributed to electron trapping/detrapping in the AlTiO. Figure 4 shows the time constants and the prefactors as functions of  $V_G$  obtained by the fitting, where the results for the MIS-HFETs with  $L_G = 0.56$  and  $1.1 \mu\text{m}$  are also shown. We find that the time constants of  $\sim 3$  ms and  $\sim 25$  ms are independent of  $V_G$  and  $L_G$ ; we consider that these two time constants correspond to two kinds of electron traps in the AlTiO, which can be related to the Poole-Frenkel conduction mechanism [8]. On the other hand, the prefactors, which are scaled by the inverse of the gate area,  $\propto 1/L_GW$ , as a natural consequence of the law of large numbers, strongly depend on  $V_G$ . Figure 5 shows the relation between the prefactors and the sheet electron concentration  $n_s$  under the gate obtained by  $C$ - $V$  measurements. We observe increase in the prefactors with decreasing  $n_s$ , indicating that the effects of electron trapping/detrapping is dominant for the case of low channel electron concentrations. This suggests that LFN near the threshold voltage can be an indicator of the quality of gate insulators.

#### 4 Summary

We investigated LFN in AlTiO/AlGaIn/GaN MIS-HFETs. While ordinary  $1/f$  LFN spectra were observed for gate biases well above the threshold voltage, near the threshold voltage, we found spectra composed of two Lorentzians attributed to electron traps in the AlTiO with specific time constants.

#### Acknowledgment

This work was supported by JSPS KAKENHI Grant Number 26249046, 15K13348.

#### References

- [1] T. Hashizume, S. Ootomo, and H. Hasegawa, Appl. Phys. Lett. **83**, 2952 (2003).
- [2] C. Liu, E. F. Chor, and L. S. Tan, Appl. Phys. Lett. **88**, 173504 (2006).
- [3] S. Yagi, M. Shimizu, M. Inada, Y. Yamamoto, G. Piao, H. Okumura, Y. Yano, N. Akutsu, and H. Ohashi, Solid-State Electron. **50**, 1057 (2006).
- [4] H.-A. Shih, M. Kudo, and T. Suzuki, Appl. Phys. Lett. **101**, 043501 (2012).
- [5] H.-A. Shih, M. Kudo, and T. Suzuki, J. Appl. Phys. **116**, 184507 (2014).
- [6] T. Q. Nguyen, H.-A. Shih, M. Kudo, and T. Suzuki, Phys. Status Solidi C **10**, 1401 (2013).
- [7] C. Mahata, S. Mallik, T. Das, C. K. Maiti, G. K. Dalapati, C. C. Tan, C. K. Chia, H. Gao, M. K. Kumar, S. Y. Chiam, H. R. Tan, H. L. Seng, D. Z. Chi, and E. Miranda, Appl. Phys. Lett. **100**, 062905 (2012).
- [8] T. Ui, M. Kudo, and T. Suzuki, Phys. Status Solidi C **10**, 1417 (2013).
- [9] S. P. Le, T. Q. Nguyen, H.-A. Shih, M. Kudo, and T. Suzuki, J. Appl. Phys. **116**, 054510 (2014).
- [10] S. L. Romyantsev, N. Pala, M. S. Shur, R. Gaska, M. E. Levinstein, M. A. Khan, G. Simin, X. Hu, and J. Yang, J. Appl. Phys. **88**, 6726 (2000).

Table I: Summary of Hooge parameter  $\alpha$ , mobility  $\mu$ , and sheet electron concentration  $n_s$  for the ungated part with and without AlTiO.

	with AlTiO	without AlTiO
$\alpha$	$\sim 4 \times 10^{-4}$	$\sim 5 \times 10^{-4}$
$\mu$ [ $\text{cm}^{-2}/\text{Vs}$ ]	1400	1500
$n_s$ [ $\text{cm}^{-2}$ ]	$9 \times 10^{12}$	$9 \times 10^{12}$

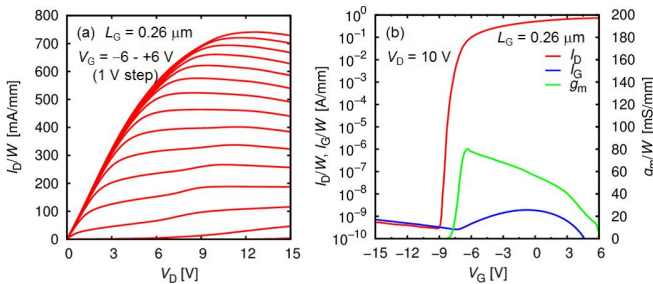


Fig. 1: (a) Output and (b) transfer characteristics of the AlTiO/AlGaIn/GaN MIS-HFET with the gate length  $L_G = 0.26 \mu\text{m}$ . Drain current  $I_D$ , gate current  $I_G$ , and transconductance  $g_m$ , all normalized by the gate width  $W$ , are shown.

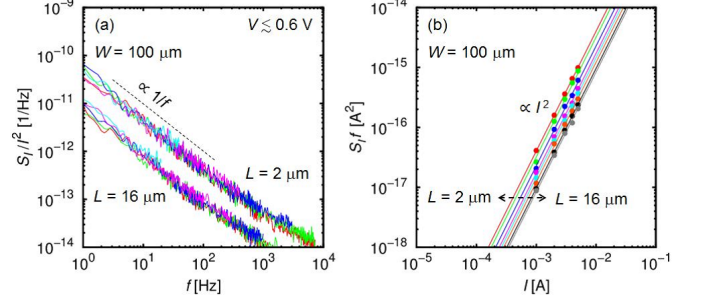


Fig. 2: (a)  $S_I/I^2$  as a function of  $f$  and (b)  $S_I f$  as a function of  $I$  for the two-terminal ungated devices.

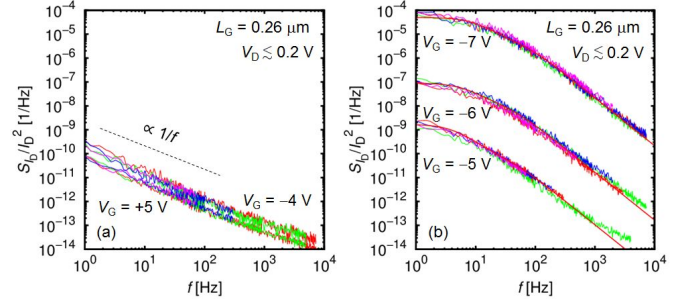


Fig. 3:  $S_{ID}/I_D^2$  as a function of  $f$  for the linear regime of the MIS-HFETs with the gate length  $L_G = 0.26 \mu\text{m}$  under the fixed gate voltages  $V_G$ .

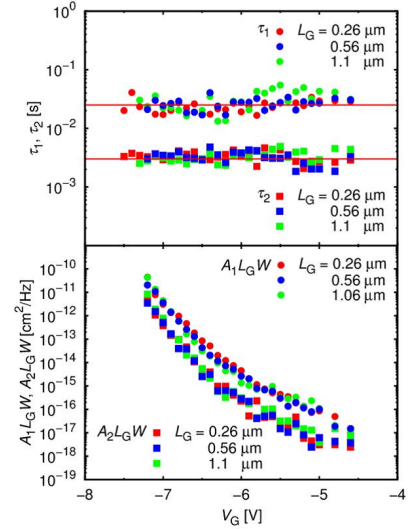


Fig. 4: (a) Time constants  $\tau_1$  and  $\tau_2$ , (b)  $A_1 L_G W$  and  $A_2 L_G W$ , as functions of  $V_G$ .

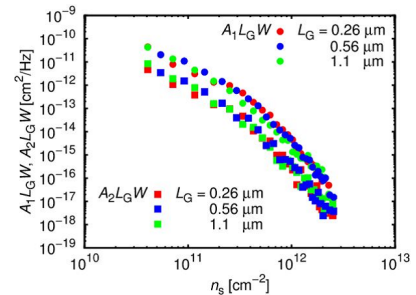


Fig. 5:  $A_1 L_G W$  and  $A_2 L_G W$  as functions of  $n_s$ .